ARTICLE
Journal of Cellular Biochemistry 114:1738–1743 (2013)

Journal of Cellular Biochemistry

Specific Route Mapping Visualized With GFP of Single-File Streaming Contralateral and Systemic Metastasis of Lewis Lung Carcinoma Cells Beginning Within Hours of Orthotopic Implantion

Babak Rashidi,[1,2] Abdool R. Moossa,[2] and Robert M. Hoffman[1,2*]

[1] *AntiCancer, Inc., San Diego, California 92111*

[2] *Department of Surgery, University of California, San Diego, California 92103-8220*

ABSTRACT

In this study, we visualized the origin of Lewis lung carcinoma metastasis after transducing tumor cells with green fluorescent protein (GFP) and transplanting them orthotopically in the middle lobe of the right lung of nude mice. Metastasis was visualized in live tissue at single cell resolution by GFP-expression as early as 18 h post-tumor transplant. At this time, single-file streaming lung carcinoma cells already had invaded inferiorly via a tubular lymphatic structure crossing the lower lobes of the lung to the ipsilateral diaphragmatic surface. By post-implantation day 2, the ipsilateral lower lobes of the lung were involved with metastatic cells. By post-implantation day 3, the ipsilateral lower lobes of the lung and the ipsilateral diaphragmatic surface were highly involved with streaming metastatic cells trafficking in single file. By Day 4 post-implantation, cancer cells invaded across the diaphragm to the contralateral diaphragmatic surface. Metastatic cells then invaded superiorly through a lymphatic vessel to involve the contralateral mediastinal lymph nodes. In this model of lung cancer, the origin of metastasis was an inferior invasion from the implanted tumor via a lymphatic duct to the ipsilateral diaphragmatic surface. The cancer cells from this site invaded on the surface of the diaphragm to the contralateral diaphragmatic surface and proceeded superiorly through a lymphatic duct to contralateral lymph nodes. Other organs such as the kidneys and the adrenal glands later became involved with metastasis with the contralateral mediastinal lymph nodes as the source. The use of GFP and the highly metastatic orthotopic lung cancer model allowed the visualization of the origin of metastasis at the single-cell level and demonstrated the critical role of lymphatic ducts and the diaphragmatic surface as the path to the contralateral side. J. Cell. Biochem. 114: 1738–1743, 2013.

KEY WORDS: GFP; LEWIS LUNG CARCINOMA; NUDE MICE; ORTHOTOPIC; IMAGING; METASTASIS; LYMPHATICS; CONTRALATERAL; DIAPHRAGM

The treatment or prevention of metastatic cancer depends on knowledge of the mode of spread [Baird, 1965]. One of the most important routes of lung cancer metastasis is via the lymphatic pathway. However, the lymphatic spread of lung carcinoma is poorly understood. Rouvière [1932] reported that lymphatic drainage of the upper lobe of both lungs is ipsilateral. However, the left middle and the left lower lobes were drained into the contralateral, right mediastinal lymph nodes [Rouvière, 1932]. In 1942, Warren and Drinker supported Rouvière's conclusions. Nohl [Nohl, 1956, 1962] and Baird [1965] also reported that in both lungs, the principal lymphatic pathway is ipsilateral. Baird [1965] mentioned that contralateral lymphatic chain metastases can occur. However, he did not explain how tumor cells reached the contralateral side. Onuigbo [1962, 1964] reported that tumors in the right lower lobe can metastasize into the left mediastinal lymph nodes. Onuigbo, however, did not describe the pathway of tumor invasion. These studies indicated that tumors in the lower lobes of both lungs are most likely able to metastasize into the contralateral mediastinal lymph nodes, but did not describe the route from the ipsilateral to the contralateral side.

We have previously demonstrated that surgical orthotopic implantation (SOI) of tumor fragments allows the full metastatic potential of tumors to be expressed [Fu et al., 1991, 1992; Furukawa et al., 1993a,b; Hoffman, 1999]. Our hypothesis was that the Lewis lung carcinoma had far greater metastatic potential than has previously demonstrated. In order to investigate the metastatic

Conflict of interest: None.

*Correspondence to: Robert M. Hoffman, AntiCancer, Inc., 7917 Ostrow Street, San Diego, CA 92111.
E-mail: all@anticancer.com

Manuscript Received: 30 January 2013; Manuscript Accepted: 4 February 2013
Accepted manuscript online in Wiley Online Library (wileyonlinelibrary.com): 26 February 2013
DOI 10.1002/jcb.24516 • © 2013 Wiley Periodicals, Inc.

potential of Lewis lung carcinoma, the tumor was transplanted to nude mice using SOI in the present study. To fully visualize metastases in the SOI Lewis lung carcinoma model, it was transduced with the green fluorescent protein (GFP) gene [Rashidi et al., 2000; Hoffman, 2005; Hoffman and Yang, 2006a,b,c; Hoffman, 2012].

The use of GFP and the highly metastatic orthotopic lung cancer model allowed the visualization of the origin of metastasis at the single-cell level and demonstrated the critical role of lymphatic ducts and the diaphragmatic surface as the path to the contralateral side. Other organs such as the brain, kidneys and the adrenal glands later became involved with metastases with the contralateral mediastinal lymph nodes as the source.

MATERIALS AND METHODS

GFP DNA EXPRESSION VECTOR

The retroXpress vector GFP pLEIN was purchased from Clontech Laboratories, Inc. (Palo Alto, CA). The pLEIN vector expresses enhanced GFP and the neomycin resistance gene on the same bicistronic message, which contains an IRES site [Rashidi et al., 2000; Hoffman and Yang, 2006a,b,c; Hoffman, 2012].

GFP VECTOR PRODUCTION

PT67, an NIH3T3-derived packaging cell line expressing the 10 Al viral envelope, was purchased from Clontech Laboratories, Inc. PT67 cells were cultured in DMEM (Irvine Scientific, Santa Ana, CA) supplemented with 10% heated-inactivated fetal bovine serum (Gemini Bio-products, Calabasas, CA). For vector production, packaging cells (PT67), at 70% confluence, were incubated with a precipitated mixture of DOTAP reagent (Roche Diagnostics, Basel, Switzerland) and saturating amounts of pLEIN plasmid for 18 h. Fresh medium was replenished at this time. The cells were examined under fluorescence microscopy after 48 h. For selection of GFP transductants, the cells were cultured in the presence of 500–2,000 μg/ml of G418 (Life Technologies, Inc., Grand Island, NY) for 7 days [Hoffman and Yang, 2006a,b,c; Hoffman, 2012].

GFP TRANSDUCTION OF LEWIS LUNG CARCINOMA CELLS

Confluent Lewis lung carcinoma cells, from the National Cancer Institute, were incubated with a 1–1 precipitated mixture of retroviral supernatants of PT67 cells and RPMI 1640 (Life Technologies, Inc.) containing 10% fetal bovine serum (Gemini Bio-Products) for 72 h. Fresh medium was replenished at this time. Lewis lung carcinoma cells were harvested by trypsin/EDTA 72 h after infection and subcultured at a ratio of 1:15 into selective medium that contained 200 μg/ml G418. The level of G418 was increased to 400 μg/ml gradually. Lewis lung carcinoma clones highly expressing GFP were isolated with cloning cylinders (Bel-Art Products, Pequannock, NJ) by trypsin EDTA and were amplified and transferred by conventional culture methods [Hoffman and Yang, 2006a, b, c; Hoffman, 2012].

MICE

Nude mice (AntiCancer, Inc., San Diego, CA) were used for these studies. Mice were housed in a HEPA-filtered barrier facility and fed with an autoclaved laboratory rodent diet. All animal studies were conducted in accordance with the principles and procedures outlined in the NIH Guide for the Care and the Use of Laboratory Animals under Assurance number A3873-1.

SUBCUTANEOUS TUMOR TRANSPLANTATION OF GFP-LEWIS LUNG CELLS

BALB/c nu/nu female mice, 6 weeks of age, were injected s.c. with a single dose of 5×10^6 of Lewis lung-GFP cells previously selected in G418 as described above. Cells were first harvested by trypsinization and washed three times with cold serum free medium and then injected in a total volume of 0.2 ml within 40 min of harvesting.

SURGICAL ORTHOTOPIC IMPLANTATION (SOI) OF GFP-LEWIS LUNG TISSUE FRAGMENTS

Tumor fragments (1 mm) derived from the Lewis lung-GFP s.c. tumors growing in nude mice were implanted by SOI on the right lung in 10 nude mice [Wang et al., 1992; Hoffman, 1999]. The mice were anesthetized by isoflurane inhalation (Fisher Sci., Hanover Park, IL). The animals were put in a position of left lateral decubitus. A 0.8-cm transverse incision of skin was made in the right chest wall. Chest muscles were separated by sharp dissection, and costal and intercostal muscles were exposed. A 0.5 cm intercostal incision between the third and fourth rib on the chest wall was made, and the chest wall was opened. The right lung was taken up by a forceps, and one tumor fragment was sewn promptly into the upper lung using one 8-0 suture. The lung was then returned into the chest cavity. The incision of the chest wall was closed with a 6-0 surgical suture. Closure of the chest wall was examined immediately and, if a leak existed, it was closed by additional sutures. After closing the chest wall, an intrathoracic puncture was made by using a 3 ml syringe and 25-gauge ½ ml needle to withdraw the remaining air in the chest cavity. After the withdrawal of air, a completely inflated lung could be seen through the thin chest wall of the mouse. The skin and chest muscles were then closed using a 6-0 surgical suture in one layer. All procedures of the operation described above were performed under a 7× microscope (Olympus).

SKIN-FLAP WINDOW

Cancer cells in the lung were visualized through the chest wall via a skin-flap window. The animals were anesthetized with the ketamine mixture. An arc-shaped incision was made and s.c. connective tissue was separated to free the skin flap. The skin flap could be opened repeatedly to image cancer cells in the lung through the nearly transparent chest wall and simply closed with a 6-0 suture. This procedure greatly reduced the scatter of fluorescent photons [Yang et al., 2002; Yamamoto et al., 2003a,b,c].

ANALYSIS OF GFP-LEWIS LUNG CARCINOMA METASTASES

After tumor progression in the SOI animals, the performance of the mice began to decrease, at which time the animals were sacrificed and autopsied. The orthotopic primary tumor and all major organs were explored under fluorescence microscopy for metastatic cells.

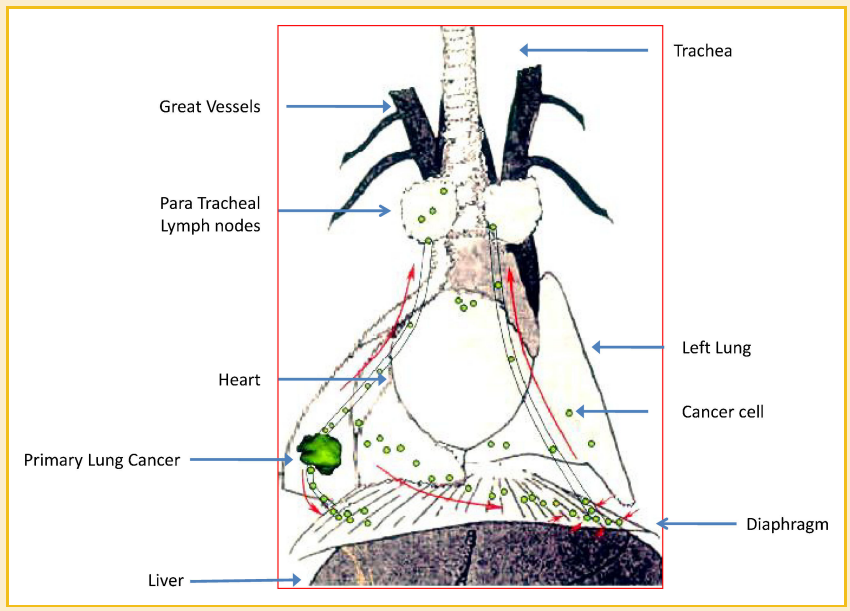

Fig. 1. A schematic of the implantation and subsequent metastasis of the Lewis lung carcinoma.

FLUORESCENCE MICROSCOPY

Fluorescence microscopy were carried out using a Nikon microscope (Melville, NY) equipped with a xenon lamp power supply. A Leica stereo fluorescence microscope model LZ12 (Buffalo Grove, IL) equipped with a mercury lamp power supply was also used. Both microscopes had a GFP filter set (Chroma Technology, Brattleboro, VT).

RESULTS AND DISCUSSION

ORIGIN OF METASTATIC PROGRESSION OF LEWIS LUNG CARCINOMA

A schematic of the implantation and subsequent metastasis of the Lewis lung carcinoma is presented in Figure 1. Eighteen hours after SOI of the Lewis lung carcinoma into the right lung, cancer cells were visualized streaming inferiorly to the ipsilateral diaphragmatic surface via a lymphatic vessel (Fig. 2).

At Day 3 post SOI, large numbers of malignant cells invaded caudally via a lymphatic vessel to the diaphragmatic surface (Fig. 3).

By Day 4 post-SOI, massive numbers of metastatic cells from the post-caval lobe of the right lobe had reached the contralateral diaphragmatic surface (Fig. 4). A few metastatic cells reached the contralateral lung through a bronco-vascular peduncle of the left lung. The heart was also involved at this time. By day 4, the cancer cells had invaded the contralateral metastatic lung (Fig. 5).

At Day 6 post-SOI, metastatic cells from the left contralateral diaphragmatic surface, invaded the left superior mediastinal lymph nodes through a lymphatic duct which connects the diaphragmatic surface and the superior mediastinal lymph nodes (Fig. 6).

At Day 3 post-SOI, the primary tumor implanted into the middle lobe of the right lung could be visualized through a skin flap over the chest wall (Fig. 7).

Mice examined at autopsy showed metastatic involvement of the brain and heart as well as throughout the mediastainal, contralateral diaphragmatic surface (Fig. 8) as well as kidneys, adrenal glands, and liver.

In this study, we were able to visualize the origin of lung cancer metastasis which involved the following stages: (1) Metastatic cells mainly invaded in the caudal direction to reach the diaphragmatic surface, (2) Contralateral mediastinal lymph-node invasion was superior from the contralateral diaphragmatic surface and is independent of contralateral lung metastases which involved a minor route via a vascular-lymphatic peduncle.

The major advantage of GFP-expressing cancer cells is that even single cells can be visualized in vivo [Hoffman, 2005, 2012;

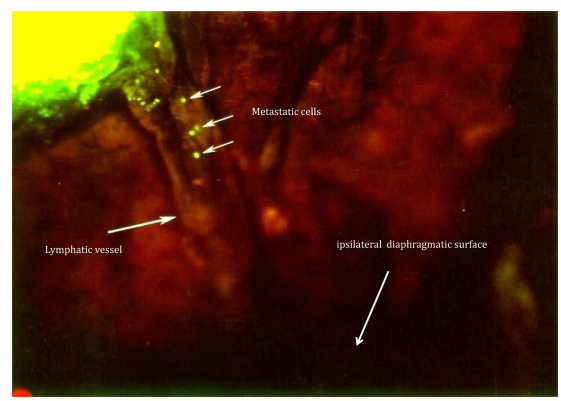

Fig. 2. Eighteen hours after SOI of the Lewis lung carcinoma into the right lung, mice were imaged for GFP-expressing Lewis lung carcinoma cells. At this time, cells were visualized streaming inferiorly to the ipsilateral diaphragmatic surface via a lymphatic vessel.

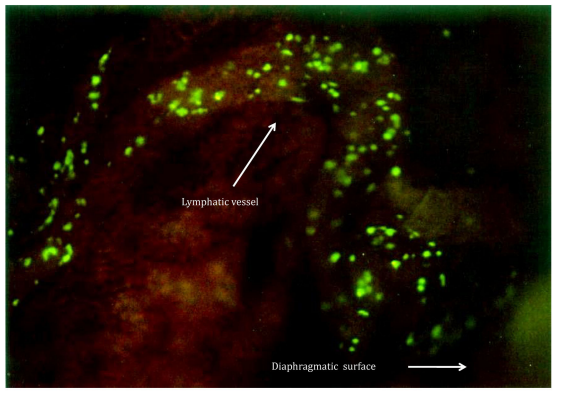

Fig. 3. At Day 3 post-SOI, large numbers of cancer cells invaded caudaly via a lymphatic vessel to the diaphragmatic surface.

Fig. 5. By 4 days post-SOI, cancer cells have invaded the contralateral metastatic lung.

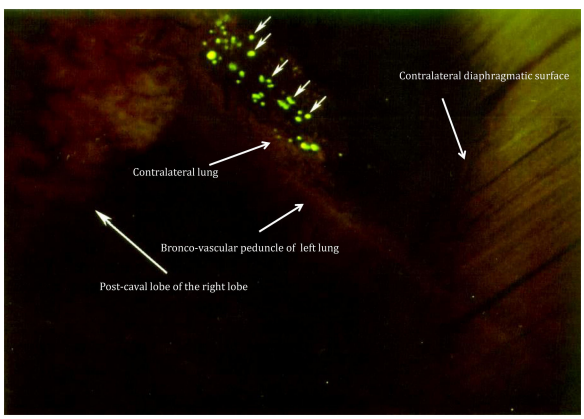

Fig. 4. By Day 4 post-SOI, massive numbers of cancer cells from the post-caval lobe of the right lobe had reached the contralateral diaphragmatic surface. A few metastatic cells reached the contralateral lung through a bronco-vascular peduncle of the left lung. The heart was also involved at this time.

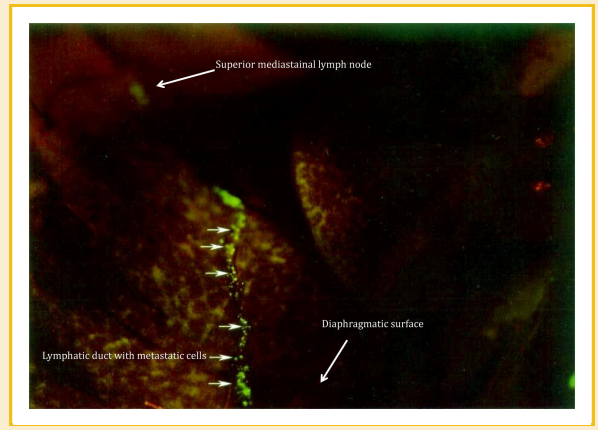

Fig. 6. At Day 6 post-SOI, metastatic cells from the left contralateral diaphragmatic surface, invaded the left superior mediastinal lymph nodes through a lymphatic duct which connects the diaphragmatic surface and the superior mediastinal lymph nodes.

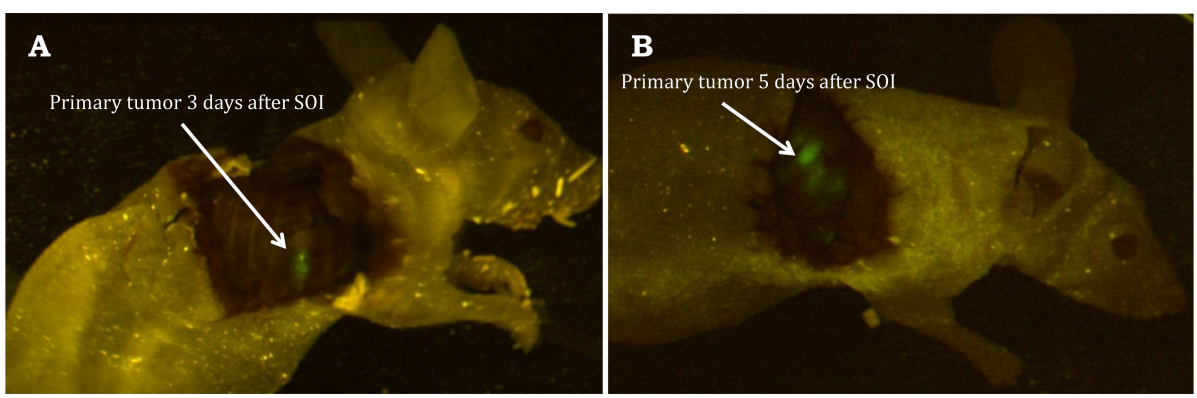

Fig. 7. At Day 3 post-SOI, the primary tumor implanted into the middle lobe of the right lung could be visualized through a skin flap over the chest wall. A: Three days after implantation. B: Five days after implantation.

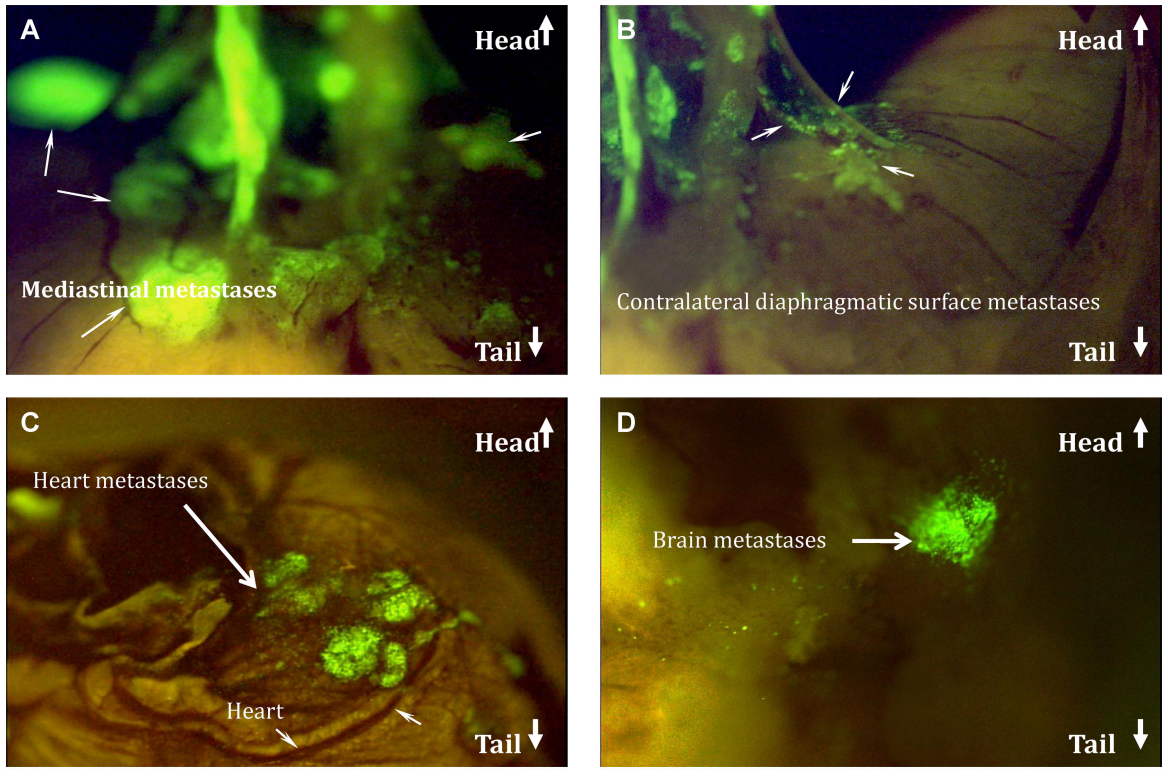

Fig. 8. Mice examined at autopsy showed metastatic involvement of the brain and heart as well as throughout the mediastainal, contralateral diaphragmatic surface as well as kidneys, adrenal glands, and liver. At Day 14 post-SOI, contralateral lung metastases became visible through the chest wall. A: Mediastinal metastases. B: Contralateral diaphragmatic surface metastases. C: Heart metastasis. D: Brain metastases.

Hoffman and Yang, 2006a,b,c; Yang et al., 2007]. The bright fluorescence and high resolution enabled us to follow the streaming of single malignant cells metastasizing to distal sites starting from the early hours after tumor implantation through the late stage of tumor progression and metastasis. An interesting question is why the metastatic Lewis lung carcinoma cells take this route. Possibly, specific affinity exists between the cancer cells, lymphatic vessels, diaphragmatic surface, and lymph nodes as well as the lung. Knowledge of the route requirements of metastatic cancer cells could lead to novel therapeutic targets whereby agents block the metastatic routes.

SURVIVAL OF ANIMALS

Starting 10 days after SOI, mice started to decline in physical activity. Animals had an average survival of 11 days. All animals died by Day 15 post-implantation.

The use of GFP and the highly metastatic orthotopic lung cancer model allowed the visualization of the origin and routes of metastasis at the single-cell level and demonstrated the critical role of lymphatic ducts and the diaphragmatic surface as the path of streaming single file cancer cells metastasizing to the contralateral side.

REFERENCES

Baird J. 1965. The pathways of lymphatic spread of carcinoma of the lung. Br J Surg 52:868–875.

Fu X, Besterman JM, Monosov A, Hoffman RM. 1991. Models of human metastatic colon cancer in nude mice orthotopically constructed by using histologically intact patient specimens. Proc Natl Acad Sci USA 88:9345–9349.

Fu X, Guadagni F, Hoffman RM. 1992. A metastatic nude-mouse model of human pancreatic cancer constructed orthotopically from histologically intact patient specimens. Proc Natl Acad Sci USA 89:5645–5649.

Furukawa T, Fu X, Kubota T, Watanabe M, Kitajima M, Hoffman RM. 1993a. Nude mouse metastatic models of human stomach cancer constructed using orthotopic implantation of histologically intact tissue. Cancer Res 53:1204–1208.

Furukawa T, Kubota T, Watanabe M, Kitajima M, Hoffman RM. 1993b. A novel "patient-like" treatment model of human pancreatic cancer constructed using orthotopic transplantation of histologically intact human tumor tissue in nude mice. Cancer Res 53:3070–3072.

Hoffman RM. 1999. Orthotopic metastatic mouse models for anticancer drug discovery and evaluation: A bridge to the clinic. Invest New Drugs 17:343–359.

Hoffman RM. 2005. The multiple uses of fluorescent proteins to visualize cancer in vivo. Nat Rev Cancer 5:796–806.

Hoffman RM, Yang M. 2006a. Subcellular imaging in the live mouse. Nat Protoc 1:775–782.

Hoffman RM, Yang M. 2006b. Color-coded fluorescence imaging of tumor-host interactions. Nat Protoc 1:928–935.

Hoffman RM, Yang M. 2006c. Whole-body imaging with fluorescent proteins. Nat Protoc 1:1429–1438.

Hoffman RM, editor. 2012. In vivo cellular imaging using fluorescent proteins: Methods and Protocols. In: Walker JM, series editor. Methods in Molecular Biology, Vol. 872. New York: Human Press (Springer Science + Business Media).

Nohl HC. 1956. An investigation into the lymphatic and vascular spread of carcinoma of the bronchus. Thorax 11:172–185.

Nohl HC. 1962. The spread of the carcinoma of the bronchus. London: Lloyd-Luke.

Onuigbo WI. 1962. Contralateral cervical node metastases in lung cancer. Thorax 17:201–204.

Onuigbo WI. 1964. Lymph node metastases in lung cancer. Geriatrics 19:380–388.

Rashidi B, Yang M, Jiang P, Baranov E, An Z, Wang X, Moossa AR, Hoffman RM. 2000. A highly metastatic Lewis lung carcinoma orthotopic green fluorescent protein model. Clin Exp Metastasis 18:57–60.

Rouvière H. 1932. Anatomie des lymphatiques de l'humme. Paris: Masson; chapters 15–17 (lymphatic system of the thorax).

Wang X, Fu X, Hoffman RM. 1992. A new patient-like metastatic model of human lung cancer constructed orthotopically with intact tissue via thoracotomy in immunodeficient mice. Int J Cancer 51:992–995.

Yamamoto N, Yang M, Jiang P, Tsuchiya H, Tomita K, Moossa AR, Hoffman RM. 2003a. Real-time GFP imaging of spontaneous HT-1080 fibrosarcoma lung metastases. Clin Exp Metastasis 20:181–185.

Yamamoto N, Yang M, Jiang P, Xu M, Tsuchiya H, Tomita K, Moossa AR, Hoffman RM. 2003b. Real-time imaging of individual fluorescent protein color-coded metastatic colonies in vivo. Clin Exp Metastasis 20: 633–638.

Yamamoto N, Yang M, Jiang P, Xu M, Tsuchiya H, Tomita K, Moossa AR, Hoffman RM. 2003c. Determination of clonality of metastasis by cell-specific color-coded fluorescent-protein imaging. Cancer Res 63:7785–7790.

Yang M, Baranov E, Wang J-W, Jiang P, Wang X, Sun F-X, Bouvet M, Moossa AR, Penman S, Hoffman RM. 2002. Direct external imaging of nascent cancer, tumor progression, angiogenesis, and metastasis on internal organs in the fluorescent orthotopic model. Proc Natl Acad Sci USA 99:3824–3829.

Yang M, Jiang P, Hoffman RM. 2007. Whole-body subcellular multicolor imaging of tumor-host interaction and drug response in real time. Cancer Res 67:5195–5200.